Dentomaxillofacial Radiology (2019) 48, 20180267
© 2019 The Authors. Published by the British Institute of Radiology
birpublications.org/dmfr

RESEARCH ARTICLE

Investigating the effect of dental implant materials with different densities on radiotherapy dose distribution using Monte-Carlo simulation and pencil beam convolution algorithm

[1]Oya Akyol, [2]Bahar Dirican, [3]Turkay Toklu, [4]Hakan Eren and [5]Turan Olgar

[1]Department Radiation Oncology, Faculty of Medicine, Gazi University, Ankara, Turkey; [2]Radiation Oncology Department, Gülhane Faculty of Medicine, Health Sciences University, Ankara, Turkey; [3]Department of Nuclear Medicine, Faculty of Medicine, Yeditepe University, Istanbul, Turkey; [4]Department of Dentomaxillofacial Radiology, Faculty of Dentistry, Ankara University, Ankara, Turkey; [5]Faculty of Engineering, Department of Physics Engineering, Ankara University, Ankara, Turkey

Objectives: The aim of this study was to investigate the effect of dental implant materials with different physical densities on dose distribution for head and neck cancer radiotherapy planning.
Methods: Titanium (Ti), Titanium alloy (Ti-6Al-4V), Zirconia (Y-TZP), Zirconium oxide (ZrO_2), Alumina (Al_2O_3) and polyetheretherketone (PEEK) dental implant materials were used for determination of implant material effect on dose distribution. Dental implant effect was investigated by using pencil beam convolution (PBC) algorithm of Eclipse treatment planning systems (TPS) and Monte Carlo (MC) simulation technique. 6 MV photon beam of the Varian 2300 C/D linear accelerator was simulated by EGSnrc-based BEAMnrc MC code system.
Results: Reasonable consistency was determined for percentage depth dose (PDD) curves between MC simulation and water phantom measurements at 6.4 MeV initial electron energy. The consistency between modelled linear accelerator PDD curve calculations and water-phantom PDD measurements were compatible within 1 % range. The dose increase in front of the dental implant calculated by MC simulation is in the range of 0.4–20.2%. We found by MC and PBC calculations that the differences in dose increase in front of the dental implant materials is in the range of 0.1–17.2% and is dependent on the physical density of the dental implant.
Conclusions: Dose increase for Zirconia was noted to be maximum while PEEK implant dose increase was minimum among the whole dental implant materials studied. This study revealed that the Eclipse TPS PBC algorithm could not accurately estimate the backscatter radiation from dental implant materials.
Dentomaxillofacial Radiology (2019) **48**, 20180267. doi: 10.1259/dmfr.20180267

Cite this article as: Akyol O, Dirican B, Toklu T, Eren H, Olgar T. Investigating the effect of dental implant materials with different densities on radiotherapy dose distribution using Monte-Carlo simulation and pencil beam convolution algorithm. *Dentomaxillofac Radiol* 2019; **48**: 20180267.

Keywords: dental Implant; Monte Carlo; radiotherapy; pencil beam convolution algorithm

Introduction

Radiotherapy is one of the most commonly used treatment modalities for head and neck cancer patients. Many of these patients have dental implants which are fixed prostheses that cannot be removed by the patient.[1]

Dental implants are made of metal, ceramic and polymer materials.[2] The use of titanium (Ti) and titanium alloy (Ti-6Al-4V) dental implants is accepted as the gold-standard in dental implantology.[3] In recent

Correspondence to: Mr Turan Olgar, E-mail: olgar@eng.ankara.edu.tr
Received 13 July 2018; revised 17 December 2018; accepted 11 January 2019

years, dental implants made of zirconium material have been used as an alternative to titanium. Zirconia (Y-TZP) and polyetheretherketone (PEEK) have not yet been used in routine clinical practice, but studies on its clinical use have been carried out.[3,4] Dental implants are usually manufactured from materials with high density.[5] Due to their high atomic number and densities, they cause problems in obtaining dose distribution in radiotherapy planning.[6] These materials cause dose scattering and dose changes around the implant during radiotheraphy.[7] In radiotherapy planning of patients with head and neck cancer, when high-energy photons interact with materials with high atomic number and high density, the radiation scattered from these materials causes soft and hard tissue complications in the mouth. These complications increase the risk of mucositis and osteoradionecrosis in patients.[8] The algorithms used for dose calculations in treatment planning systems (TPS) cannot accurately calculate the scattered dose.[9] The Monte Carlo (MC) simulation is the best way to model the radiation beam and its interactions. More accurate results are obtained in dose calculations using MC simulation.[1,5,9]

Several groups have made measurements to investigate dental implant materials effect on the dose distribution. Ozen et al[8] and Beyzadeoglu et al[10] evaluated dose increment related to scattered radiation from bone-dental implant surface and beam incidence angle. Catlı[9] evaluated high-density dental implant effect on dose distribution and compared Monte Carlo simulation with pencil beam convolution (PBC) algorithm of Eclipse TPS. Chang et al[11] and De Conto et al[1] evaluated backscatter dose increment on mucosa depending on physical density and electron density of metal crown. Spiridovich et al evaluated high-density dental implant effect on dose distribution by comparing MC simulation with Pinnacle TPS.[5]

The aim of this study is to investigate the effect of dental implant materials with different densities on dose distribution for head and neck radiotherapy planning. The effect of Ti, Ti-6Al-4V, Y-TZP, Zirconium oxide (ZrO_2), Alumina (Al_2O_3) and PEEK dental implant materials on dose distribution was studied by using the PBC algorithm of Eclipse TPS and MC simulation technique and the results obtained by the PBC algorithm and the MC simulation were compared.

Methods and materials

Physical properties of different dental implant materials

In this study, six commercial dental implants were used: Ti, Ti-6Al-4V, Y-TZP, ZrO_2, Al_2O_3 and PEEK. The chemical compositions, physical densities (g/cm³) and electron densities (electron/cm³) of these materials are given in (Table 1)[2,3,9,11–15]

The electron densities (ρ_e) are calculated from chemical compositions of the materials using following equation,

$$\rho_e = \rho N_A \sum \frac{w_i Z_i}{A_i} \quad (1)$$

Where ρ is the physical density, N_A is Avogadro's number ($6.022 \times 10^{23}\ mol^{-1}$), A_i and Z_i is the atomic weight and atomic number of the ith element and w_i is its percentage fraction by weight.

Relative electron densities were calculated by dividing the electron densities of the materials to that of water.[16] The relative electron densities of Ti, Ti-6Al-4V,Y-TZP, ZrO_2, Al_2O_3 and PEEK dental implant materials are 3.76, 3.71, 4.62, 4.65, 3.50, 1.25 respectively.

Treatment planning system

The Eclipse TPS (v. 8.6.15, Varian Medical Systems, Palo Alto, CA) is a three-dimensional conformal radiotherapy dose calculation system. The Eclipse TPS dose calculations utilize PBC algorithm and three different inhomogeneity corrections.[17] In this study, dosimetric calculations were performed using the PBC algorithm and modified batho power law (MBPL) inhomogeneity correction. Eclipse TPS uses CT transformation tables that convert CT number information to electron density while performing dose calculations.

The phantoms were created for six different dental implant materials for dose calculations in Eclipse TPS. Each dental implant material was placed into solid water phantom which has dimension of 30 × 30 × 30 cm³ at depth of 2 cm with 1 cm thickness. The phantom images used for the Eclipse TPS are shown in Figure 1.

The phantoms are scanned with CT by selection of 0.5 mm slice thickness. CT images were transferred to Eclipse Software (v. 8.6.15, Varian Medical Systems, Palo Alto, CA). The dental implant materials in each

Table 1 Chemical compositions, physical and electron densities of different dental implant materials

Materials	*Common name*	*Chemical composition*	*Physical density (g/cm³)*	*Relative electron density*
H2O	Water	H,O	1.00	1.00
Titanium	Ti	Ti	4.54	3.76
Titanium alloy	Ti-6Al-4V	Ti,Al,V	4.34	3.72
Zirconia	Y-TZP	Zr,Y,O	6.01	4.62
Zirconium oxide	ZrO2	Zr,O	5.68	4.65
Alumina	Al2O3	Al,O	3.97	3.50
Polyetheretherketone	PEEK	C,H,O	1.30	1.25

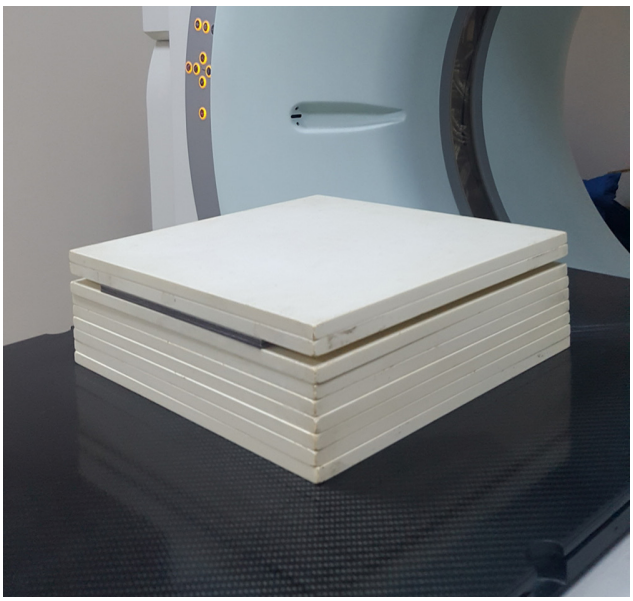


Figure 1 The phantom geometry used in the Eclipse TPS.

CT slice image were manually contoured for dose calculations. The electron density values corresponding to the Hounsfield unit (HU) values of the Ti, Ti-6Al-4V,Y-TZP, ZrO_2, Al_2O_3 implant materials were manually entered to the CT number—electron density conversion table in the Eclipse TPS.[9,16] Electron density values for PEEK are available in the TPS system. Phantoms' dose plans were generated by using 6 MV photon beam in Eclipse TPS, because 6 MV photon beam is usually used in treatment of head and neck cancer patients. Dose calculations for phantoms were carried out with 10 × 10 cm² field size and source surface distance (SSD) of 100 cm. Percentage depth dose (PDD) curves were obtained along the central axis as center of the implant material is isocenter. All doses were normalized by the dose at depth of 1.5 cm.

Monte Carlo simulation

The photon beam of 6 MV nominal-energy of the Varian 2300 C/D linear accelerator was simulated by EGSnrc-based BEAMnrc (v. 2010) MC code system.[18,19] Head geometry of the system was modelled by using manufacturer's specifications (Varian Medical Systems, Palo Alto, CA). Target, primary collimator, vacuum window, flatting filter, ion chamber, mirror, jaws, multileaf collimators (MLCs) were simulated using SLABS, CONS3R, SLABS, FLATFILT, CHAMBER, MIRROR, JAW and VARMLC component modules (CMs) of BEAMnrc, respectively.

To determine electron beam characteristics incident to the target, only the mean energy of initial electron beam was considered as an adjustable parameter while energy and radial intensity distribution of the beam were kept constant. Circular electron beam source with 2 mm full-width at half-maximum (FWHM) Gaussian radial intensity distribution in both X and Y directions and 1 MeV FWHM Gaussian energy distribution were set using source number 19 of BEAMnrc.[20,21] Phase–space (PhSp) files were produced at the end of the accelerator head for the electron beams of mean energy from 5.4 to 6.6 MeV with 0.2 MeV increment using BEAMnrc code. The initial number of electrons hit to the target was 2×10^9 for 10 × 10 cm² field size. The cut-off energies for electrons and photons were set as 0.7 and 0.01 MeV, respectively. The variance reduction technique of directional Bremsstrahlung splitting (DBS) with a splitting number of 1000 was used to increase computational efficiency.[22]

PhSp files were used as initial source in DOSXYZnrc code.[23] A 40 × 40 × 40 cm³ sized water phantom with 0.4 × 0.4 × 0.4 cm³ voxels was created in the code. Three-dimensional dose distributions, PDD and profile curves were obtained for each initial electron beam energy. Three-dimensional dose files produced by DOSXYZnrc in "*.3ddose" format were then read with the DICOM-RT toolbox in MATLAB™.[24]

The results of each simulation were compared with the ionization chamber measurements carried out with PTW ionization chamber (PTW 31010 semiflex, Germany) in water tank (PTW MP3, Germany). The mean energy that best matches with the ionization chamber measurements was selected as initial electron beam energy for the other simulations performed in the study.

Phantoms with 30 × 30 × 20 cm³ dimensions were created in DOSXYZnrc for each dental implant material to calculate the dose distributions. Voxel sizes of the phantoms were 0.3 × 0.3 × 0.2 cm³ and the dimension of 0.2 cm was towards the direction of the photon beam. Each dental implant material with 1 cm thickness was placed into water phantom at depth of 2 cm (Figure 2).

The physical densities and chemical compositions of the implant materials were added to 700ICRU.pegs4dat

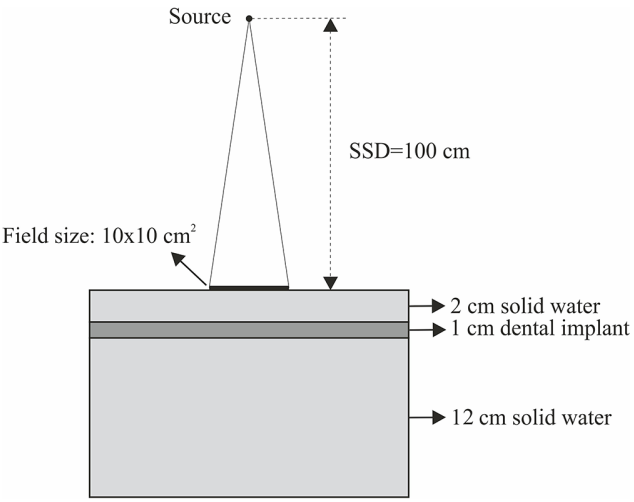


Figure 2 The phantom geometry used in the DOSXYZnrc for MC simulation. MC,Monte Carlo; SSD, source surface distance.

PEGS4 (Preprocessor for Electron γ Shower) file supplied with the code system and the cross-sectional data was generated from this file. The PhSp file generated with selected mean electron energy for 10 × 10 cm^2 field was used in phantom dose calculations. The initial numbers of histories were adjusted to keep statistical uncertainty less than 0.5%.

DICOM-RT toolbox was used to read 3D dose distributions.[24] The isocenter was set as center of the dental implant material and PDDs were calculated along the central axis. All doses were normalized by dose value at 1.5 cm depth.

Dose enhancement in front of the implant material due to the backscattering effect and dose decrement behind implant material because of the absorption for six different dental implant materials were calculated with MC simulations.

Data comparison and analysis

The difference between the dose values calculated from the PDD curves by the Eclipse TPS PBC algorithm and the MC simulation were calculated by using following equation:

$$Difference\,(\%) = \left[\left(D_{MC} - D_{PBC}\right)/D_{MC}\right] \times 100 \qquad (2)$$

Results

PDD and dose profile curves for MC simulation of each beam energy were compared with water phantom measurements for 10 × 10 cm^2 field and SSD:100 cm. The best consistency between MC simulation and water phantom measurement results was noted at 6.4 MeV initial electron energy. The compatibility between these results is 1%. Comparisons between MC simulations and water phantom measurements is shown in Figure 3.

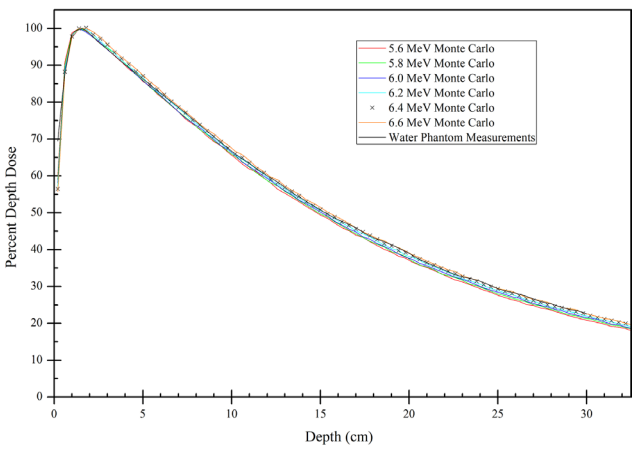


Figure 3 Comparisons between the PDD curves of water phantom measurement and MC simulations with different initial energies for 10 × 10 cm^2 field and SSD:100 cm. MC,Monte Carlo; PDD, percentage depth dose.

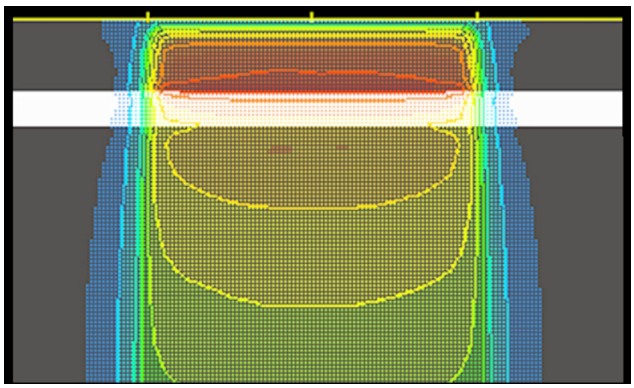


Figure 4 Dose distribution obtained by MC simulation for Ti implant. MC,Monte Carlo.

The dose distribution obtained by MC simulation and Eclipse TPS PBC algorithm for Ti dental implant material is shown in Figures 4 and 5, respectively.

The results obtained from the PDD curves were used to explain the effect of different implant materials on dose distributions. The PDD curves obtained by comparing MC simulation technique and the Eclipse TPS PBC algorithm for different dental implant materials are shown in Figures 6–11. Each implant material was placed at a depth of 2 cm.

The calculated dose increment and decrement by MC simulation in front of and behind the dental implant is given in Table 2. The percentage dose differences were calculated between PDD curves of MC simulation and Eclipse TPS PBC algorithm. The dose differences were calculated in front of, just behind, 2 cm behind and 10 cm behind of different dental implant materials and the results are given in Table 3.

From MC and PBC calculations, we found that the differences in dose increase in front of the dental implant materials are in the range of 0.1–17.2% and is dependent on the physical density of the dental implant.

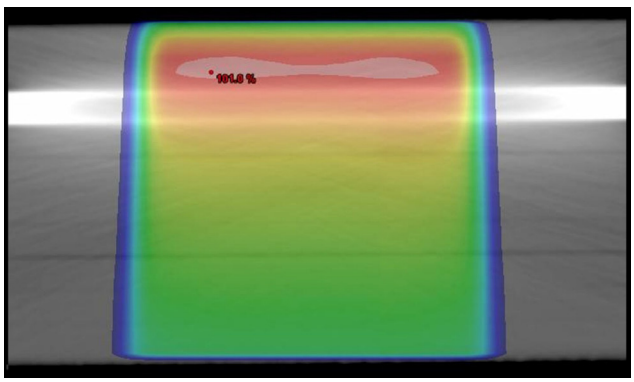


Figure 5 Dose distribution obtained by Eclipse TPS PBC algorithm for Ti implant. PBC,pencil beam convolution; TPS, treatment planning systems.

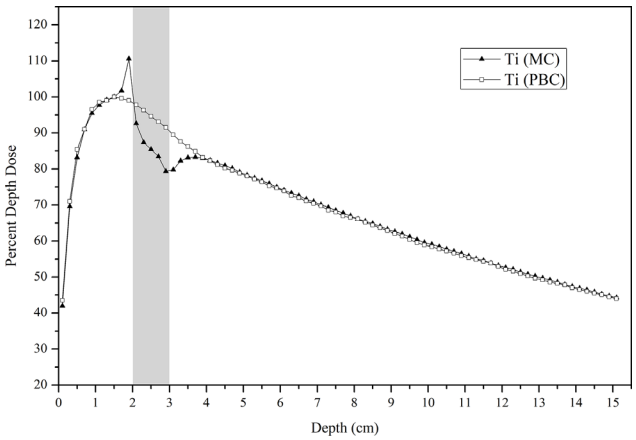


Figure 6 Comparisons between the PDD curves obtained by MC simulations and PBC algorithm for Ti implant at 6 MV. PBC,pencil beam convolution; PDD, percentage depth dose; TPS, treatment planning systems.

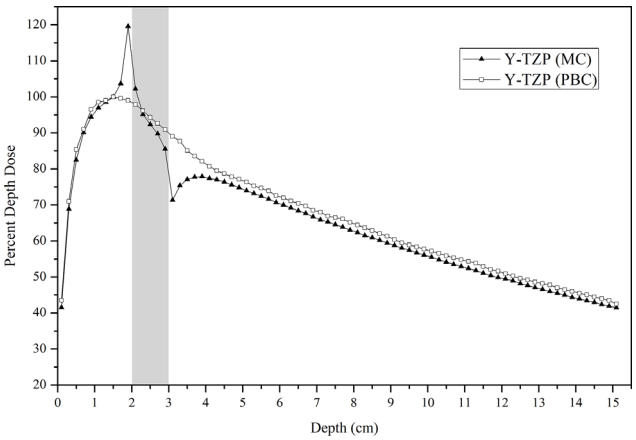


Figure 8 Comparisons between the PDD curves obtained by MC simulations and PBC algorithm for Y-TZP implant at 6 MV. PBC,pencil beam convolution; PDD, percentage depth dose; TPS, treatment planning systems.

Discussion

In this study, MC simulation of the treatment head of Varian 2300 C/D was carried out successfully. EGSnrc/BEAMnrc and DOSXYZnrc were accepted as the accurate MC code system. The calculated PDD and beam dose profiles were in good agreement with ionization chamber measurements by water phantom.

The calculated dose increment by MC simulation in front of dental implant is 11.2% for Ti, 10.7% for Ti-6Al-4V, 20.2% for Y-TZP, 15.5% for ZrO_2, 3.3% for Al_2O_3 and 0.4% for PEEK. The dose increment is mainly related to the electron density of the materials. The real dose increase was determined by MC simulation. The PBC algorithm does not take the dose increment in front of the dental implant related to backscatter into consideration. Catlı[9] and Friedrich et al[25] studied the backscatter dose increment by using MC simulation. The reported dose increment in front of the implant by Catli was 7.8% for Ti and 6.3% for Ti-6Al-4V.[9] Friedrich et al also observed 10% dose increment in front of the Ti implant.[25] The results obtained in this study for the Ti implant material are consistent with that reported by Friedrich et al. The difference between our results and that reported by Catlı for Ti and Ti-6Al-4V implant material might arise from the beam simulation. We simulated the real beam by taking the parameter of the head of the Linac into consideration, whereas Catli[9] used standard 6 MV beam.

To the best of our knowledge, there is no comparative study in the literature for the four different dental implant materials (Y-TZP, ZrO_2, Al_2O_3,PEEK) used in this study.

The maximum dose increment was observed for the Zirconia implant, because the implant material has the highest physical density. The lowest dose increase is found for the PEEK implant because of the PEEK implant material has the lowest physical density.

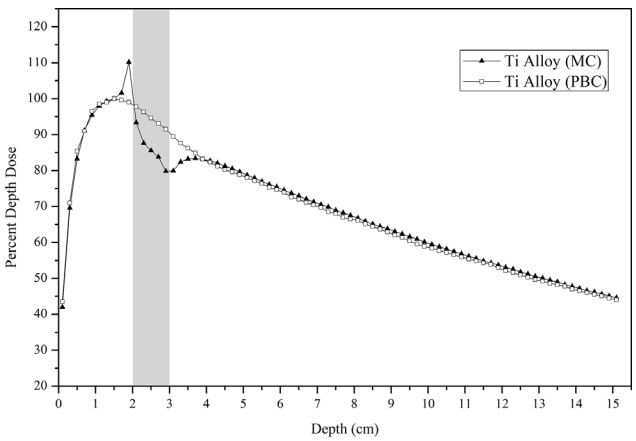


Figure 7 Comparisons between the PDD curves obtained by MC simulations and PBC algorithm for Ti alloy implant at 6 MV. PBC,pencil beam convolution; PDD, percentage depth dose; TPS, treatment planning systems.

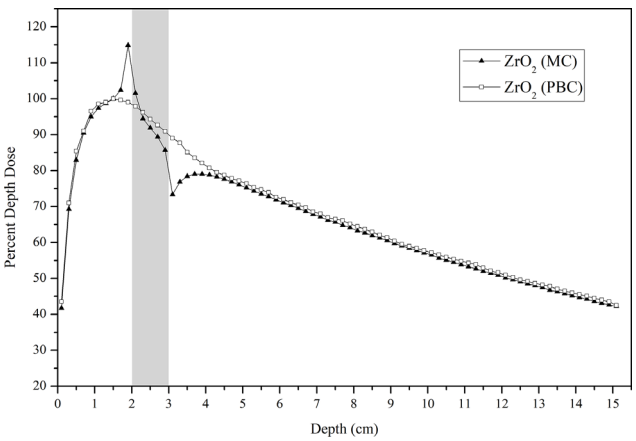


Figure 9 Comparisons between the PDD curves obtained by MC simulations and PBC algorithm for ZrO_2 implant at 6 MV. PBC,pencil beam convolution; PDD, percentage depth dose; TPS, treatment planning systems.

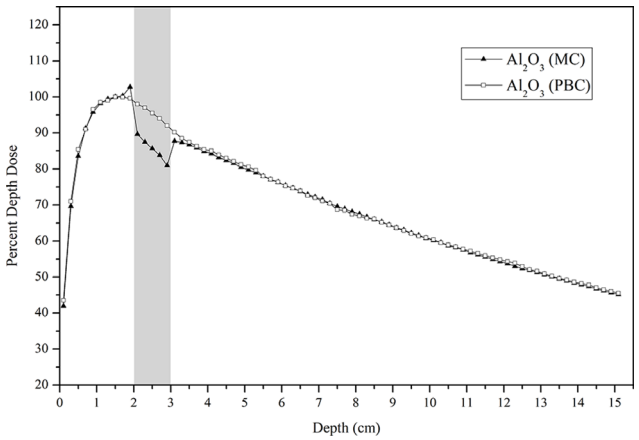


Figure 10 Comparisons between the PDD curves obtained by MC simulations and PBC algorithm for Al_2O_3 implant at 6 MV. PBC,pencil beam convolution; PDD, percentage depth dose; TPS, treatment planning systems.

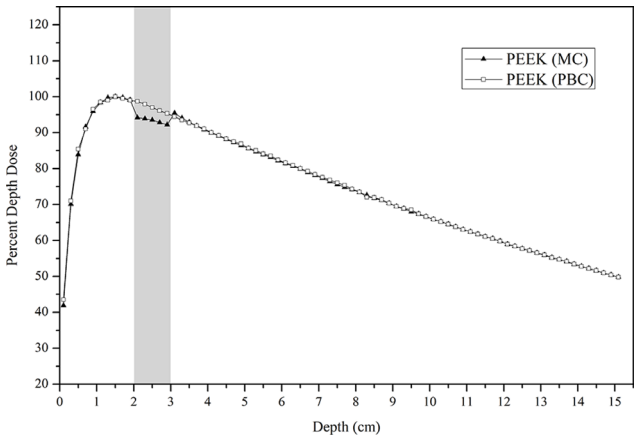


Figure 11 Comparisons between the PDD's of the results obtained by MC simulations and PBC algorithm for PEEK implant at 6 MV. PBC,pencil beam convolution; PDD, percentage depth dose; TPS, treatment planning systems.

The increase in the dose in front of the implant material due to back scattering is proportional with the increase in the density of the material. The reason of this increase is obvious; the Compton interaction is almost independent of the atomic number of the material but proportional to the density of the material.[26] The dose increase is due to the scattering of the secondary electrons on the material.

Comparison of PDD curves obtain by MC simulations and Eclipse TPS PBC algorithm calculations shows that the dose increment difference in front of the dental implant is 10.5% for Ti,10.1% for Ti-6Al-4V, 17.2% for Y-TZP, 13.8% for ZrO_2, 3.1% for Al_2O_3 and 0.1% for PEEK. The difference between calculated dose decrement with MC simulation and PBC algorithm at 6 MV beam is 12.2% for Ti, 12% for Ti-6Al-4V, 24.7% for Y-TZP, 21.3% for ZrO_2, 2.7% for Al_2O_3 and 0.9% for PEEK. Comparison of PDD curves obtained with MC simulations and Eclipse TPS PBC algorithm calculations shows that the TPS PBC algorithm can not accurately calculate the scattering and absorption of dental implant materials for small inhomogeneous mediums.

Treatment planning algorithms give dose calculations more accurately for radiation interaction with the homogeneous medium. In this study, it was seen that the dose was reduced behind the implant materials due to absorption, while the dose was increased in front of implant materials due to back scattering. PBC algorithm underestimated the backscatter dose in front of the dental implant and overestimated the dose behind the dental implants.

PBC algorithm could not calculate dose accurately, because it does not take the lateral scattering into account. The PBC algorithm calculates the dose accurately for homogeneous mediums such as water. Some errors were reported in dose calculations for inhomogeneous medium with this algorithm.[27] The MC simulation takes the physical densities and chemical compositions of the materials into account in dose calculations. The

Table 2 The calculated dose increase and dose decrease (%) by MC simulation at 6 MV beam for different dental implant materials

	Ti	*Ti-6Al-4V*	*Y-TZP*	*ZrO_2*	*Al_2O_3*	*PEEK*
The backscatter dose in front of dental implant	11.2	10.7	20.2	15.5	3.3	0.4
The dose decrement just behind the dental implant	15.5	15.4	24.4	22.2	7.0	1.1

PEEK, polyetheretherketone.

Table 3 The calculated dose difference (%) between MC simulation and PBC algorithm at 6 MV beam for different dental implant materials.

	Ti	*Ti-6Al-4V*	*Y-TZP*	*ZrO_2*	*Al_2O_3*	*PEEK*
The backscatter dose in front of dental implant	10.5	10.1	17.2	13.8	3.1	0.1
The dose decrement difference just behind the dental implant	12.2	12.0	24.7	21.3	2.7	0.9
The dose decrement difference behind the dental implant at 2 cm distance	0.4	1.0	3.4	1.6	1.1	0.1
The dose decrement difference behind the dental implant at 10 cm distance	1.0	1.8	3.4	1.5	0.4	0.2

PEEK, polyetheretherketone.

MC simulation is shown to give most accurate and reliable dose calculations for inhomogeneous material.[28]

Intensity modulated photon radiotherapy is currently being used to avoid xerostomia and several other radiotherapy-related morbidities by the dose deposited in the beam path.[29] However, the proton radiotherapy is currently being used for cancer management and allows less adjacent healthy tissue exposure with establishing minimized side-effects especially in salivary glands and taste buds compared to photon radiotherapy.[30]

Conclusion

In this study, dose distribution effects on head and neck radiotherapy planning of different implant materials were investigated using Eclipse TPS PBC algorithm and MC simulation methods. We can conclude that from the dose calculation results obtained in this study, the PBC algorithm is inadequate for dose calculations in inhomogeneous medium with high-density materials. The MC simulation gives more accurate and reliable results when compared with PBC algorithm of Eclipse TPS.

The established dose increase with MC simulation in front of different dental implant materials is between 0.4 and 20.2%. The difference between dose increase calculated with MC simulation and PBC algorithm of Eclipse TPS is in the range of 0.1–17.2% in front of the material within the treatment area depending on the physical density of the dental implant materials. Tissue complication caused by high-density implant materials has been shown by several studies. It is unclear whether a maximum 20.2% dose increase causes increased mucositis and osteoradionecrosis complication risk.[8] It is recommended that dental implant materials which would not cause tissue complication should be preferred for patients regarding to possibilities having head and neck cancer in future. MC-based algorithms should be used in head and neck radiotherapy planning to estimate the dose increase accurately for different high-density dental implant materials.

Acknowledgment

This work was partially supported by The Scientific and Technological Research Council of Turkey (TUBITAK) grant (216S166).

REFERENCES

1. De Conto C, Gschwind R, Martin E, Makovicka L. Study of dental prostheses influence in radiation therapy. *Phys Med* 2014; **30**: 117–21. doi: https://doi.org/10.1016/j.ejmp.2013.03.002
2. Osman RB, Swain MV. A critical review of dental implant materials with an emphasis on titanium versus zirconia. *Materials* 2015; **8**: 932–58. doi: https://doi.org/10.3390/ma8030932
3. Özkurt Z, Kazazoğlu E, implants Zdental, literature review A. Zirconia dental implants: a literature review. *J Oral Implantol* 2011; **37**: 367–76. doi: https://doi.org/10.1563/AAID-JOI-D-09-00079
4. Schwitalla AD, Spintig T, Kallage I, Müller WD. Flexural behavior of peek materials for dental application. *Dent Mater* 2015; **31**: 1377–84. doi: https://doi.org/10.1016/j.dental.2015.08.151
5. Spirydovich S, Papiez L, Langer M, Sandison G, Thai V. High density dental materials and radiotherapy planning: comparison of the dose predictions using superposition algorithm and fluence MAP Monte Carlo method with radiochromic film measurements. *Radiother Oncol* 2006; **81**: 309–14. doi: https://doi.org/10.1016/j.radonc.2006.10.010
6. AAPM Tissue inhomogeneity corrections for megavoltage photon beams, Report no. AAPM-85. *AAPM Task Group No. 65 of the Radiation Therapy Committee. Madison, WI: Med Phys. Publishing* 2004.
7. Wang R, Pillai K, Jones PK. Dosimetric measurement of scattered radiation from dental implants in simulated head and neck radiotherapy. *See comment in PubMed Commons below Int J Oral Maxillofac Implants* 1998; **13**: 197–203.
8. Ozen J, Dirican B, Oysul K, Beyzadeoglu M, Ucok O, Beydemir B. Dosimetric evaluation of the effect of dental implants in head and neck radiotherapy. *Oral Surgery, Oral Medicine, Oral Pathology, Oral Radiology, and Endodontology* 2005; **99**: 743–7. doi: https://doi.org/10.1016/j.tripleo.2004.11.048
9. Çatli S. High-density dental implants and radiotherapy planning: evaluation of effects on dose distribution using pencil beam convolution algorithm and Monte Carlo method. *J Appl Clin Med Phys* 2015; **16**: 46–52. doi: https://doi.org/10.1120/jacmp.v16i5.5612
10. Beyzadeoglu M, Dirican B, Oysul K, Ozen J, Ucok O. Evaluation of scatter dose of dental titanium implants exposed to photon beams of different energies and irradiation angles in head and neck radiotherapy. *Dentomaxillofac Radiol* 2006; **35**: 14–17. doi: https://doi.org/10.1259/dmfr/28125805
11. Chang K-P, Lin W-T, Shiau A-C, Chie Y-H. Dosimetric distribution of the surroundings of different dental Crowns and implants during linac photon irradiation. *Radiation Physics and Chemistry* 2014; **104**: 339–44. doi: https://doi.org/10.1016/j.radphyschem.2013.11.026
12. Abd El-Ghany OS, Sherief AH. Zirconia based ceramics, some clinical and biological aspects: review. *Future Dental Journal* 2016; **2**: 55–64. doi: https://doi.org/10.1016/j.fdj.2016.10.002
13. Coplen TB. Atomic weights of the elements 1999 (IUPAC technical Report.). International Union of pure and applied chemistry, inorganic Chemistry division, Commission on atomic weights and isotopic abundances. *Pure Appl. Chem* 2001; **73**: 667–83.
14. Khare N, Limaye PK, Soni NL, Patel RJ. Friction and wear characteristics of peek and peek composites in water lubricated slow speed sliding. *Tribology Online* 2015; **10**: 84–90. doi: https://doi.org/10.2474/trol.10.84
15. Piconi C, Maccauro G. Zirconia as a ceramic biomaterial. *Biomaterials* 1999; **20**: 1–25. doi: https://doi.org/10.1016/S0142-9612(98)00010-6
16. Coolens C, Childs PJ. Calibration of CT Hounsfield units for radiotherapy treatment planning of patients with metallic hip prostheses: the use of the extended CT-scale. *Phys Med Biol* 2003; **48**: 1591–603. doi: https://doi.org/10.1088/0031-9155/48/11/308
17. Chaikh A, Giraud JY, Balosso J. Practical and applied medical physics: clinical comparison of density correction methods associated with pencil beam convolution algorithm for clinical situations. *Med Phys International Journal* 2014; **2**: 49–53.

18. Kawrakow I. Accurate condensed history Monte Carlo simulation of electron transport. I. EGSEGSnrc, the new EGS4 version. *Med Phys* 2000; **27**: 485–98. doi: https://doi.org/10.1118/1.598917
19. Rogers DW, Faddegon BA, Ding GX, Ma CM, We J, Mackie TR. Beam: a Monte Carlo code to simulate radiotherapy treatment units. *Med Phys* 1995; **22**: 503–24. doi: https://doi.org/10.1118/1.597552
20. Rogers DWO, Walters B, Kawrakow I, Manual B. National Research Council of Canada (NRCC) Report PIRS-0509(A) revL. 2017.
21. Sheikh-Bagheri D, Rogers DW. Sensitivity of megavoltage photon beam Monte Carlo simulations to electron beam and other parameters. *Med Phys* 2002; **29**: 379–90. doi: https://doi.org/10.1118/1.1446109
22. Kawrakow I, Rogers DW, Walters BR. Large efficiency improvements in BEAMnrc using directional bremsstrahlung splitting. *Med Phys* 2004; **31**: 2883–98. doi: https://doi.org/10.1118/1.1788912
23. Kawrakow I, Walters BR. Efficient photon beam dose calculations using DOSXYZnrc with BEAMnrc. *Med Phys* 2006; **33**: 3046–56. doi: https://doi.org/10.1118/1.2219778
24. Spezi E, Lewis DG, Smith CW. A DICOM-RT-based toolbox for the evaluation and verification of radiotherapy plans. *Phys Med Biol* 2002; **47**: 4223–32. doi: https://doi.org/10.1088/0031-9155/47/23/308
25. Friedrich RE, Todorovic M, Todrovic M, Krüll A. Simulation of scattering effects of irradiation on surroundings using the example of titanium dental implants: a Monte Carlo approach. *Anticancer Res* 2010; **30**: 1727–30.
26. Bushberg JT, Seibert JA, Leidholdt EM, Boone JM. *The Essential Physics of Medical Imaging*. Third Edition. Philadelphia: Lippincott Williams&Wilkins; 2012.
27. Li JS, Pawlicki T, Deng J, Jiang SB, Mok E, Ma CM, JS L, CM M. Validation of a Monte Carlo dose calculation tool for radiotherapy treatment planning. *Phys Med Biol* 2000; **45**: 2969–85.
28. Lu L. Dose calculation algorithms in external beam photon radiation therapy. *Int J Cancer Ther Oncol* 2013; **1**: 01025. doi: https://doi.org/10.14319/ijcto.0102.5
29. Sipahi C, Beyzadeoglu M, Demirtas S, Ozen J. Effect of different mucosal and acrylic resin surface treatments in a denture retention model for patients with radiotherapy-induced xerostomia. *Int J Prosthodont* 2007; **20**: 405–8.
30. Deshpande TS, Blanchard P, Wang L, Foote RL, Zhang X, Frank SJ. Radiation-related alterations of taste function in patients with head and neck cancer: a systematic review. *Curr Treat Options Oncol* 2018; **19**: 72. doi: https://doi.org/10.1007/s11864-018-0580-7